

Article

# The Niger River Basin Moisture Sources: A Lagrangian Analysis

Rogert Sorí <sup>1,\*</sup>, Raquel Nieto <sup>1,2</sup>, Anita Drumond <sup>1</sup> and Luis Gimeno <sup>1</sup>

<sup>1</sup> Environmental Physics Laboratory (EPhysLab), Facultad de Ciencias, Universidade de Vigo, Ourense 32004, Spain; rnieto@uvigo.es (R.N.); anitadru@uvigo.es (A.D.); l.gimeno@uvigo.es (L.G.)

<sup>2</sup> Department of Atmospheric Sciences, Institute of Astronomy, Geophysics and Atmospheric Sciences, University of São Paulo, São Paulo 05508-090, Brazil

\* Correspondence: rogert.sori@uvigo.es; Tel.: +34-988-387-208

Academic Editor: Anthony R. Lupo

Received: 23 November 2016; Accepted: 9 February 2017; Published: 14 February 2017

**Abstract:** The Niger River basin (NRB) is located in the important climatic region of the African Sahel. In this study we use the Lagrangian tridimensional model FLEXPART v9.0 to identify and characterise the moisture sources for the NRB. This method allows the integration of the budget of evaporation minus precipitation over 10-day backward trajectories, thereby identifying the origins of the air masses residing over the NRB. The analysis was performed for the 35-year period from 1980 to 2014, which allowed us to identify the main semi-annual climatological moisture sources of the NRB, for November–April (NDJFMA) (dry season) and May–October (MJJASO) (wet season), and to quantify the respective moisture uptakes. Throughout the year, the NRB main moisture sources are located on the tropical eastern North Atlantic Ocean near Africa, the tropical eastern South Atlantic Ocean in the Gulf of Guinea, in the regions surrounding the Sahel and in the Mediterranean Sea. The extents of these sources vary between dry and wet seasons. In NDJFMA two regions appear in the east of the basin, which then join up, forming a larger source to the northeast of the basin in MJJASO, when three other less important moisture sources can be seen in central-equatorial Africa, the tropical western Indian Ocean and the Persian Gulf. In NDJFMA the majority of the moisture uptake comes from the NRB itself but then, later in MJJASO, when the precipitation increases over the basin the greatest uptake of moisture occurs over the tropical eastern South Atlantic Ocean, northeast Africa and the NRB, which suggests that these are the effective sources of precipitation in the basin in overall terms. The seasonal moisture uptake quantification over the moisture sources of the NRB, reveals that largest fraction of moisture income to the basin from outside its boundaries. Despite providing moisture to the NRB the source located in the tropical eastern North Atlantic Ocean does not contribute that much to precipitation in the basin. A daily (ten-day) backward analysis shows the importance of the moisture uptake within the NRB and from near moisture sources during the first few (backward) days, while the Atlantic Ocean sources and the Mediterranean became more important during the last five (backward) days of the analysis.

**Keywords:** moisture sources; Lagrangian analysis; Niger River basin

---

## 1. Introduction

Several authors have investigated the moisture sources for precipitation in the Sahel and West Africa (WA) by using a range of different methods. Rainfall over any area of land has two possible sources: water vapour advected into the region from the surrounding areas, and that which is supplied by evaporation from within the same region [1]. The identification of mechanisms and sources of moisture responsible for the precipitation regimes is crucial for the understanding of the global hydrological cycle and for improving the predictive power of numerical models [2]. In fact, the

identification of moisture sources as part of the analysis of extreme events has become a major research area (e.g., for flooding and droughts), but it is also increasingly important for regional and global climatic assessments, including paleoclimatic reconstructions and future climate change scenarios [3].

Differences in Sahelian precipitation rate are primarily a consequence of the contrasting circulation, together with recycling of local evaporation and moisture advected from the tropical North Atlantic Ocean and the Gulf of Guinea [4]. Evaporation in the tropical Atlantic Ocean, WA, and Central Africa (CA) contribute about 23%, 27%, and 17% of the total rainfall in WA [1]. Precipitation recycling is defined as the contribution of local evaporation to local precipitation [5]. Utilizing a Lagrangian method, Nieto et al. [6] investigated the moisture sources for the African Sahel in five-year period (2000–2004), confirming recycling as the dominant moisture source over the Sahel. Through a quasi-isentropic back-trajectory scheme Dirmeyer et al. [7] also obtained that terrestrial evaporative source that supplied the water for precipitation is dominant in this region.

Results of van der Ent et al. [8], using a moisture recycling approach to study the complete process of continental moisture feedback also demonstrated that the Sahel region receives its moisture from three large water bodies: the Mediterranean Sea, the South Atlantic Ocean, and the Indian Ocean, and on average about 50% to 60% of the precipitation originates from continental evaporation. The same technique, based in a water accounting model of 2-D moisture tracing and 3-D moisture tracing was implemented by Keys et al. [9,10], respectively, confirming that land surface plays a dominant role in mediating variability in moisture recycling processes for the sink region of the West Sahel. Nevertheless, evaporative source regions for precipitation in the nearby located western Sahel can probably not be diagnosed adequately using the 2-D approximation due to the strong generation of vertical inhomogeneities by surface evaporation and by directional shear [11]. On the other hand, in a recent study Arnault et al. [12] describe how local evaporation in WA is not the dominant factor controlling local precipitation over this region. These authors implemented a set of two methods (tracking of tagged atmospheric water species originating from evaporation in a source region, i.e., E-tagging, and three-dimensional budgets of total and tagged atmospheric water species) developed in the weather research and forecasting (WRF) model for investigating regional precipitation recycling mechanisms. They observed that locally-evaporated water was mainly transported outside of the target domain at the lower levels. Specifically for the Niger River basin (NRB), Stohl and James. [13] utilized a Lagrangian approach for a five-year period (1999–2003), finding that about half of the moisture provided to it originates from the Atlantic Ocean and half originates from the land (including from the NRB itself). There is also a climatology of evaporative moisture sources for the NRB, as well as their seasonal variations and mean contributions in a period of 25 years available online [14]. These results were obtained through the quasi-isentropic back-trajectory scheme utilized by Dirmeyer et al. [7], and reveal the importance of the basin itself and surrounded Sahel regions providing moisture to the basin [14]. A comparison of different methodologies to study the source-receptor relationships have been provided by Gimeno et al. [3].

As discussed, studies of moisture source identification and atmospheric transport mechanisms are fundamental for understanding the nature of the precipitation. Studies of climate variability in WA show the seasonal rainfall migration during the boreal summer [15,16] and a reduction in accumulated rainfall over the last century [17–20]. These phenomena have affected stream discharges and both are considered a partial feedback of the land-cover degradation in the watershed [21]. A review of recent studies of rainfall regime in the West African Sahel by Nicholson [22] shows some recovery since the extreme dry episodes of the 1970s and 1980s, but also certain changes in the rainfall regime, such as less spatial coherence and less temporal persistence. Investigations of the moisture sources of the NRB has become particularly important if we consider that the total population of the basin is about 130 million, 70% of whom live in rural areas [23] and most of them, as well as the economies of countries in the NRB rely mainly on agriculture, pastoral systems, crop-livestock systems and fishing [24]. This work aims to perform a climatological study to identify the moisture sources of the NRB, but take into account a longer period of time, as well as consider variations of the sources between dry and rainy seasons

in the basin. Likewise, the purpose is to emphasize on the role of each source and the NRB itself providing moisture to the basin. The results will support new climatic and hydrological research in the NRB. Particularly, they will strengthen the knowledge for understanding the mechanisms associated with the rainfall variability and the occurrence of extreme weather events in this basin.

## 2. Study Area

The Niger River basin (NRB) is located in West Africa (WA) along the Sahel region (Figure 1). It is shared by nine countries and, at 4200 km in length, the Niger River itself is the third longest in Africa after the Nile and the Congo/Zaire. The Sahel is a transition zone between the Sahara desert and the wet climate of tropical Africa [25], giving the basin contrasting climatic conditions that mainly vary with latitude. According to the climatic classification of L'Hôte and Mahé [26] for WA based on annual rainfall, the NRB experiences five climatic zones with a gradual variation between deserts (arid) in the north, to transitional equatorial in the south. The mean annual precipitation ranges from less than 50 mm/year in the northern part of the basin in Algeria, increasing southwards to more than 2000 mm/year close to the river mouth in the Guinean coastal zone [27]. In WA the mean annual cycle of precipitation, is characterised by minimum values at the beginning of the year that increase month by month, reaching a peak in August, to later decrease until December [28].

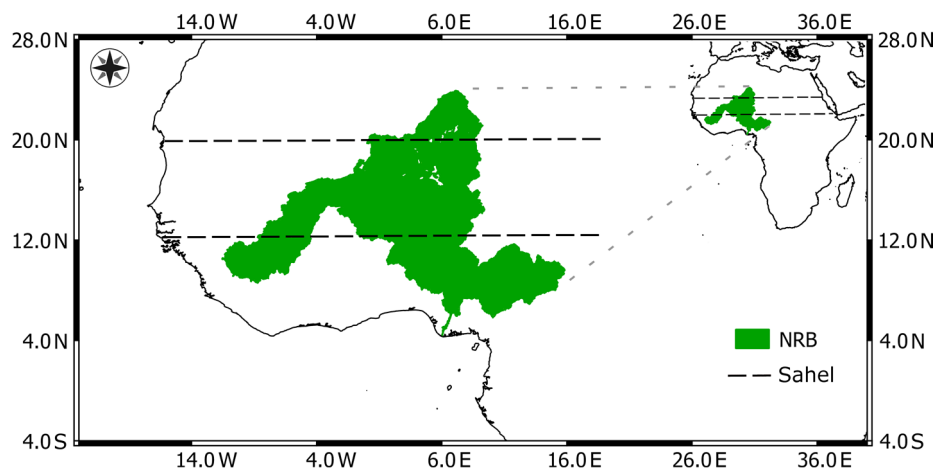


**Figure 1.** Geographical location of the Niger River Basin (green area) in West Africa.

For WA some authors consider the rainy season to be the period May–October, and the dry season to be November–April [29,30]. In fact, the maximum precipitation rate occurs from May–October and the minimum during November–April [28]. However, Andersen et al. [27] consider the periods June–November and December–May as wet and dry seasons in the basin, while Liebmann et al. [15] argue that the southern coast of WA experiences a wet season beginning in early March and its duration decreasing latitudinally to the north. During the boreal summer, an intense heat low develops over the Western Sahara [22]. This is termed the Saharan heat low (SHL) and it is the thermal response of the lower troposphere over the northern African continent to seasonal surface warming [31]. The SHL plays a pivotal role in the West African Monsoon (WAM) system in spring and summer [32]. It controls the zonal circulation of the lower half of the troposphere, particularly the westerly component of the monsoon winds and with the anticyclonic circulation around 600 hPa at the top of the heat low, it controls the speed of the African Easterly Jet (AEJ) [33]. The monsoon is longer and wetter in the southern part of the NRB [34]. In the dry season, under the influence of the Saharan high-pressure zone, the northeastward Harmattan wind brings hot, dry air and high temperatures, which last longer in the north of the basin [27].

The observed annual average precipitation varied over the period 1951–2010 over Africa, showing negative trends in some parts of the NRB [17]. The major circulation features associated with the

variability of the rainfall in the Sahel at interannual and decadal time scales are the upper-level Tropical Easterly Jet, the mid-level African Easterly Jet, and the Saharan heat low; a correlation with the intensity of the Intertropical Convergence Zone (ITCZ) (as defined by rainfall intensity) is also apparent [22]. A schematic overview of the basic surface circulation is depicted in Figure 2. It shows the sea level pressure (SLP) and winds at 1000 mb in North Africa for the seasons under study, November–April and May–October. In the dry season, high pressures observed in the north of Africa decrease with latitude and, as a result, winds flow from the northeast over the NRB towards the south, and there is a confluence of winds with those flowing from the southwest (Figure 2a). In the wet season, the surface southerly monsoon onshore flow penetrates through the rain band over the entire seasonal cycle, while the depth of the southerly surface monsoon flow undergoes some seasonal variation, being highest during the peak of the monsoon [35]. This is shown in Figure 2b: low pressures extend from the east to the West of Africa between 10° N and 25° N approximately, and winds flowing from the south turn from a southwesterly direction after crossing the equator and are dominant in the major part of the NRB until they reach its northern part, where the confluence is now located due to the weakening effect of the winds from the northeast.

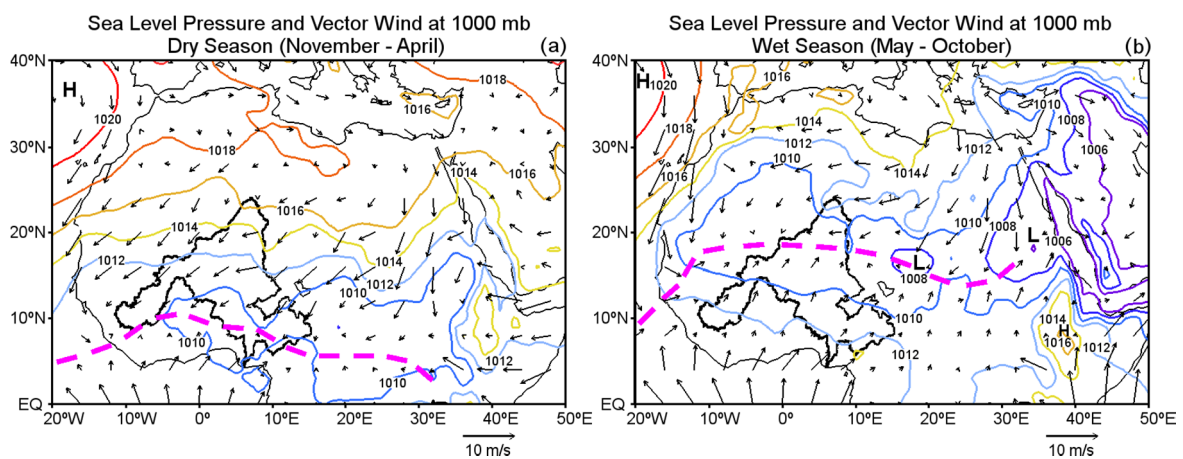


**Figure 2.** Climatological schematic diagram of mean sea level pressure (colour contours, in mb) and winds (arrows, in m/s) at 1000 mb from ERA-Interim, for the period 1980–2014 during NDJFMA (a) and MJJASO (b). The discontinued magenta line represents the confluence of winds and the black contour in West Africa indicates the boundary of the NRB.

### 3. Experiments Section

#### 3.1. Method

In this study we applied the Lagrangian particle dispersion model FLEXPART v9.0 developed by Stohl and James [13,36]. The model considers the atmosphere divided homogeneously into three-dimensional finite elements (hereafter “parcels”) over the entire globe, each representing a fraction of the total atmospheric mass [36]. This allows variations in atmospheric moisture to be obtained along backward and forward trajectories of air parcels, permitting the establishment of meaningful source-receptor relationships. In our case, a backward analysis was performed using parcels residing over the NRB, limiting the transport time to 10 days in accordance with the average residence time of water vapour in the atmosphere [37]. This way, the rate of moisture increase (through evaporation from the environment,  $e$ ) or decrease (through precipitation,  $p$ ) along the trajectory of the parcels can be calculated by changes to the specific humidity ( $q$ ) over time ( $t$ ) by Equation (1), assuming a constant mass ( $m$ ) of the particles:

$$(e - p) = m(dq/dt) \quad (1)$$

It is possible to obtain the moisture changes of all parcels in the atmospheric column over an area, obtaining the surface freshwater flux, hereafter denoted  $(E - P)$ . Nevertheless,  $q$  fluctuations along individual trajectories can occur for nonphysical reasons (e.g., because of  $q$  interpolation or trajectory errors); a limitation partly compensated among the many particles in an atmospheric column over the target area. More details about this method have been provided by Stohl and James [13,36].  $(E - P)$  is obtained from the sum of the  $(e - p)$  associated with all the particles present in the atmospheric column over the NRB. Recalling that  $(e - p)$  is proportional to the temporal variations of  $q$  in a particle during the 6-h interval. The  $(E - P)$  sign then would correspond to the prevailing  $(e - p)$  conditions associated with the particles observed in that atmospheric column during a given time interval. A region is then considered as a moisture source when  $(E - P) > 0$ , i.e., the net moisture budget of the particles tracked is favourable to the evaporation from the environment into the particles. The opposite occurs in a moisture sink, i.e., a region in which the moisture budget associated is favourable to the moisture loss by the tracked particles to the environment. For this work, to identify the moisture sources we calculated the budget of  $(E - P)$  integrated over 10 days (the mean residence time of the water vapour in the global atmosphere), meaning that  $(E - P) > 0$  or  $(E - P) < 0$  values are the result of the integrated daily  $(E - P)$  values over the 10 days. The regions in which prevailed  $(E - P) > 0$  conditions during the 10 day-period are considered moisture sources, while regions where particles lose humidity ( $(E - P) < 0$ ) are considered moisture sinks.

FLEXPART has been applied in the pursuit of similar goals in several regions of the world, including the Sahel [6], the Sahelian Sudan [38], the Orinoco River Basin [39], China [40], the Amazon River Basin [41], and several continental regions [42].

The budget of  $(E - P)$  was calculated for two semi-annual climatological periods, from November to April (NDJFMA) and from May to October (MJJASO), considered to represent the dry and rainy seasons, respectively. For both seasons the backward analysis was implemented from 1 to 10 days, and the results were then integrated over the 10 days ( $(E - P)i10$ ) to define the climatological moisture sources.

A percentile criterion was applied to the  $(E - P)i10$  field to define a threshold delimiting the spatial extent of the respective sources of moisture. The 90th percentile delimits those regions where the air masses were likely to have picked up a large amount of moisture on their transit towards the target region. In other words, the 90th percentile criteria would show the 10% grid points with the highest positive  $(E - P)i10$  values in the map. This criterion has been applied for similar purposes in Drumond et al. [41], Drumond et al. [43], and Drumond et al. [44]. The NRB itself was considered a moisture source area.

### 3.2. Data

The analyses were carried out using 35 years of data (1980–2014), ensuring that climatological results were obtained. The Lagrangian model FLEXPART is forced by the ERA Interim reanalysis datasets [45] available at 6 h intervals (00, 06, 12, and 18 UTC) at a resolution of  $1^\circ \times 1^\circ$  with 60 model layers with the top of the atmosphere located at 0.1 hPa. The ERA-Interim reanalysis achieved good progress with respect to data assimilation problems previously encountered in ERA-40, mostly related to the use of satellite data, resulting in an improved representation of the hydrological cycle, a more realistic stratospheric circulation, and better temporal consistency on a range of time-scales [45].

Datasets of precipitation in the basin from the Climatic Research Unit (CRU 3.23TS) [46] were used to calculate the annual cycle of precipitation in the NRB. This datasets available with a resolution of  $0.5^\circ \times 0.5^\circ$  were constructed from monthly observations at meteorological stations across the world's land areas [46]. To calculate the Vertically Integrated Moisture Flux (VIMF) we used datasets of the vertical integral of the eastward and northward water vapour flux from the ERA-Interim reanalysis [45] at a resolution of  $1^\circ \times 1^\circ$ .

## 4. Results and Discussion

### 4.1. Backward Analysis of ( $E - P$ )

The seasonal budget of ( $E - P$ ) backward-integrated using FLEXPART for the NRB from  $-1$  to  $-10$  days for the dry and wet seasons is shown in Figure 3. Areas where ( $E - P$ )  $> 0$  are considered evaporative regions and, thus, moisture sources, while regions where ( $E - P$ )  $< 0$  are moisture sinks. Over these regions is evident that the number of trajectories that coincide is high. This analysis makes it possible to identify those areas where air masses tracked backwards from the NRB take up humidity. Additionally, worth mentioning is that moisture sink regions (bluish colours) in Figure 3 could also act as moisture sources, since local evaporation could end up as precipitation over themselves or other regions. However, here FLEXPART has been used to compute the budget of ( $E - P$ ) just on air masses tracked backward in time from the NRB, thus representing the net freshwater flux into the air masses traveling to the target basin.

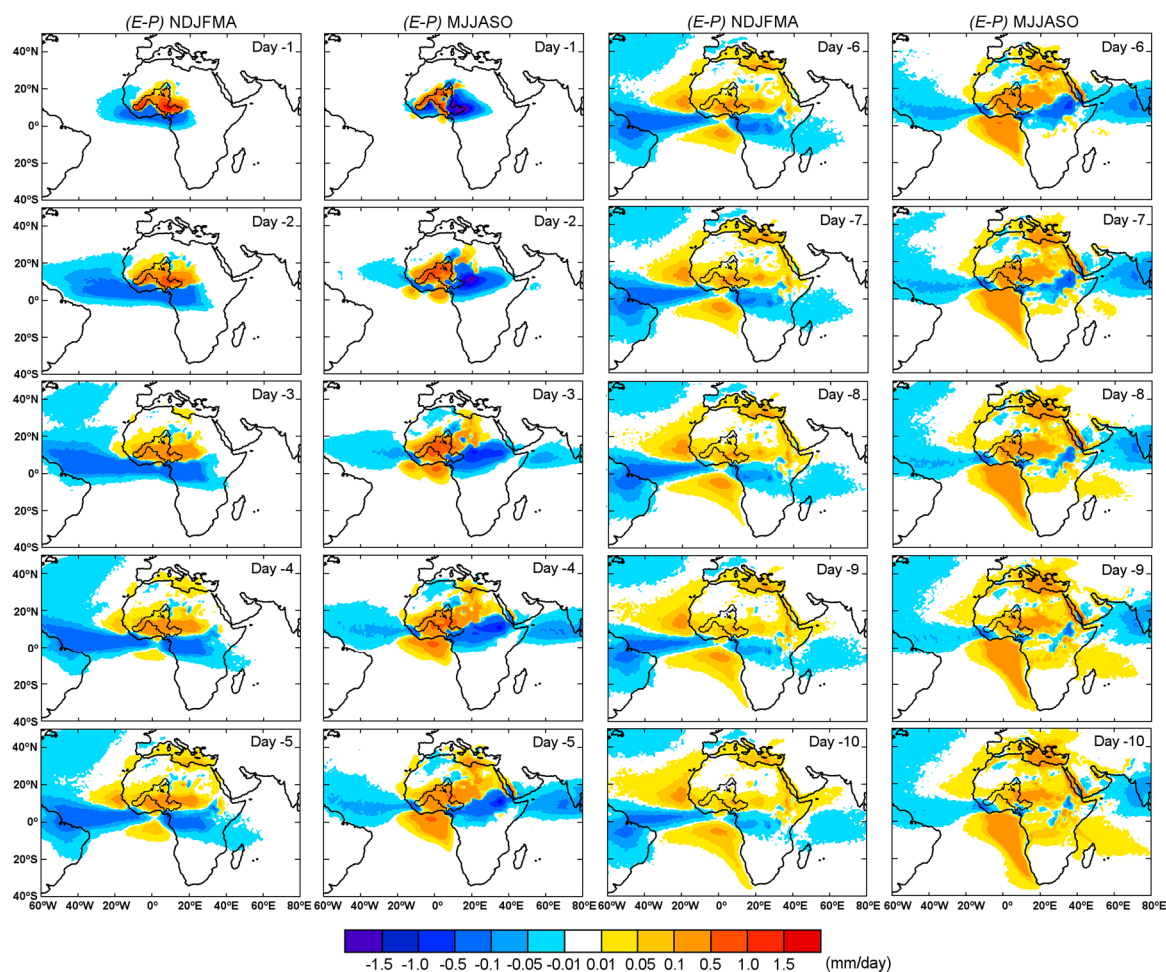


**Figure 3.** Seasonal pattern of ( $E - P$ ) backward-integrated from the Niger River Basin for days  $-1$  to  $-10$ , for dry (NDJFMA) and wet (MJJASO) seasons.

For both periods at one day backwards in time (day  $-1$ ) the NRB mainly acts as its own moisture source, but in MJJASO the eastern part of the basin and the Sahel regions that lie mostly to the east and south of the NRB act as moisture sinks, suggesting convective precipitation that typically occurs in air masses in transit to the Sahel [6]. At days 2 and 3 back in time (days  $-2$  to  $-3$ ) the pattern of ( $E - P$ ) is characterised by positive values remaining over the NRB and extending across the Sahel and North Africa, although they are also observed for MJJASO over the Gulf of Guinea in the wet

season. For these days, areas of  $(E - P) < 0$  are distributed throughout equatorial Africa and the Atlantic Ocean, but they are displaced further south in NDJFMA when the ITCZ moves to the summer hemisphere [22]. At days  $-4$  and  $-5$  the spatial pattern of  $(E - P)$  expands and both the NRB and the Sahel remain as moisture sources. The east-equatorial South Atlantic Ocean (covering the Gulf of Guinea) and the Mediterranean Sea are now moisture sources and persist throughout the remaining days of the analysis, although according to Schicker et al. [47] the western part of North Africa receives less Mediterranean rainwater than Northeast and Central Africa. Particularly on these days, the tropical-east North Atlantic Ocean becomes a much expanded moisture source in NDJFMA. For these, and all preceding days, it is commonly observed that regions where parcels lose moisture to the atmosphere before reaching the NRB are more intense around the equatorial Atlantic Ocean, Central Africa, and the Arabian Sea.

Regarding the source regions, the greatest differences observed between the  $(E - P) > 0$  areas for NDJFMA and MJJASO may be seen clearly between  $-5$  to  $-10$  days in the tropical east North Atlantic Ocean. In MJJASO the positive values in the spatial pattern are confined to the African coast but in NDJFMA they are propagated to the west until reach the Caribbean by days  $-9$  and  $-10$ . In these days it is clear that in NDJFMA uptake takes place over part of the Arabian Sea, but the opposite occurs in MJJASO when the Arabian Sea remains a moisture sink while it also becomes an important moisture source for precipitation for the Indian monsoon [48]. During the boreal summer months in the west tropical Indian Ocean between  $0^\circ$  and  $10^\circ$  S, a small region of  $(E - P) > 0$  expands to the east from day  $-6$  through to day  $-10$ , when it reaches  $20^\circ$  S.

Despite the moisture source regions varying or persisting throughout the 10 days of the analysis, part of the uptake of moisture for the NRB from these regions can fall as precipitation along the trajectories of the air masses when they move towards the target area [49]. In MJJASO when the WAM increases the rainfall in WA, the pattern of  $(E - P)$  is mostly characterised by higher values of  $(E - P) > 0$ . A common characteristic of the field of  $(E - P)$  for both seasons is the persistence of moisture contribution from the NRB itself during first few days of the backward analysis, which suggests the importance of local recycling, as previously identified as the major source of moisture for the Sahel [6].

#### 4.2. Climatological Moisture Sources Delimitation

As a means of summarising and giving proper consideration to all of the daily results, we integrated the budget of  $(E - P)$  for all 10 days backwards in time for each period, dry and wet (Figure 4). Spatial differences of resulting positive values in the budget of  $(E - P)$  confirm the importance of considering the rainfall seasonal variation in the target region to identify the moisture sources. The 90th percentile (p90) of the  $(E - P) > 0$  values is shown by the magenta line, which identifies the predominantly evaporative regions, i.e., those finally utilized as moisture sources for the NRB. These are shown more clearly in the schematic illustration in Figure 5. The p90 was calculated in a matrix for the entire globe, thus, the percentile value does not change for another domain. As commented, the boundaries of the sources delimited by the p90 values show the 10% grid points with the highest positive  $(E - P)_{i10}$  values in the map. To understand how appropriate are the boundaries of the sources delimited using this criterion, there was calculated the 80th and 95th percentiles and later plotted along with p90 over the integrated budget of  $(E - P)$  for all 10 days backwards in time, for dry and wet seasons (Supplementary Materials Figure S1). In this figure, it is easy to appreciate that between boundaries of p80 and p90,  $(E - P)_{i10} > 0$  values are low, while the threshold of p95 comprises extremely high values.

In the dry season the threshold of p90 = 0.13 mm/day (Figure 4a) defines the following boundaries of the moisture sources regions: the “tropical east north Atlantic Ocean” (NAtl), the “tropical east south Atlantic Ocean” (SAtl), the “Western Sahel” (WSah), the NRB, the “Southern Sahel” (SSah), the “Eastern Sahel” (ESah), “Eastern Africa” (EA), and the “Mediterranean” (MEDT) region that mainly comprises the Mediterranean Sea and a small part of the Northern African continent (Figure 5a). In the wet season, most of the sources selected using the threshold of p90 = 0.10 mm/day (Figure 4b)

remain the same as for the dry season, but their spatial extents change and new sources appear. It can clearly be seen that boundaries of the MEDT source are now expanded to the north over Europe, while the SATl to the south and the Natl are reduced and confined near the African coasts. To the northeast of the basin a large source (hereafter NEA) covers a wide area that even comprises part of the Red Sea. In Central Equatorial Africa a moisture source occupies a belt extending from the Atlantic to the Indian Ocean, henceforward named CEA. Other new small sources are located in the “Indian Ocean” (Ind) and the Persian Gulf (Figure 5b).

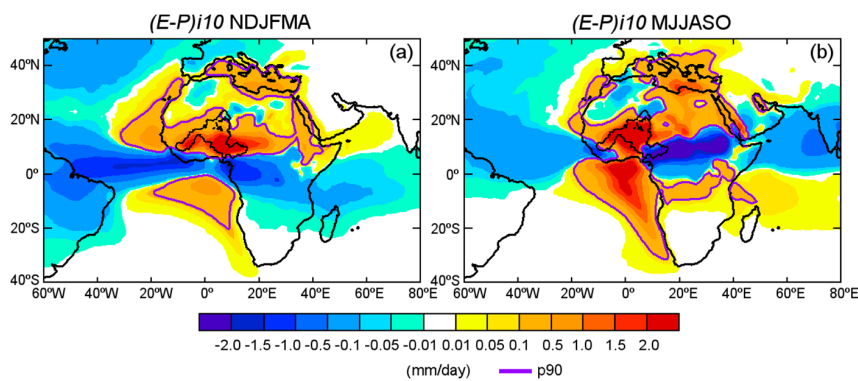


**Figure 4.** Average pattern of  $(E - P)$  backward results integrated from the Niger River Basin for all 10 days for the dry (a) and wet season (b). The magenta line represents the 90th percentile of the  $(E - P)_{i10} > 0$  values: (a)  $p90 = 0.13$  mm/day, and (b)  $p90 = 0.10$  mm/day.

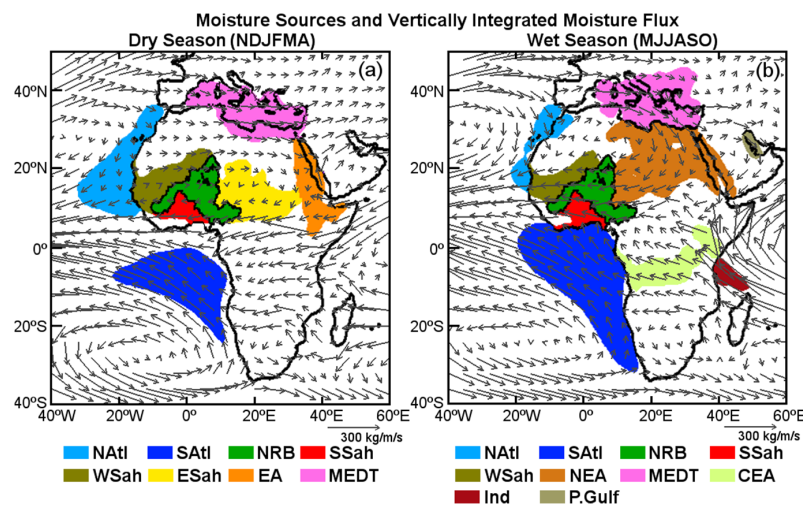


**Figure 5.** Schematic representation of moisture sources for the NRB (colour shaded areas) and average vertically integrated moisture flux (VIMF) (arrows) from ERA-Interim, for the period 1980–2014 during the dry (a) and wet (b) seasons.

A climatology of evaporative moisture sources for the NRB [14] obtained by a quasi-isentropic back-trajectory scheme highlight the importance of recycling ratio in the NRB, which agrees with our results (Figures 3 and 4). Both methods also recognise the importance on the moisture contribution to the basin from the  $(E - P) > 0$  regions represented in Figure 4. Nevertheless, our finding reflect a greatest spatial extension of the  $(E - P) > 0$  areas through the tropical-north Atlantic Ocean in the period November–April respect the period May–October, while results in the already commented climatology represent the evaporative source of the NATl extended in April–September and limited to the North African coasts in October–March. Additionally, according to Keys et al. [10] who implemented an Eulerian method for tracking moisture, the most important evaporation source regions in the ERA-I

western Sahel precipitation shed during the growing season, come from the Gulf of Guinea, the entire east-west expanse of the Sahel, the Mediterranean Sea, Central Africa, the coastal Mediterranean regions, and the Mozambique Channel. These results for the Sahel coincide greatly with those obtained in this work, but the seasonal analysis implemented in ours also reveals the seasonal spatial variability of the NRB's moisture sources.

#### 4.3. Daily Budget of $(E - P)$ Over the Sources

The daily budgets of  $(E - P)$  over the sources, obtained in the backward experiment with FLEXPART are shown in Figure 6. Positive values represent moisture uptake while the negative values show losses of moisture. Positive  $(E - P)$  values appear whether the sum of the  $(e - p)$  associated with the parcels moving over a certain area is positive. Figure 6 shows the time series of daily  $(E - P)$  calculated backward for moisture over NRB and integrated over the different sources considered. These results show the total contribution from each source, regardless of the number of parcels identified or the sources areas. To understand these values it must be noted that source areas are not spatially of the same size and, thus, the amount of moisture uptake, or lose over them are quite scale dependent. In the dry season during the first few days backwards in time (from day  $-1$  to  $-4$ ) the most important sources accounting for  $(E - P) > 0$  values, are the NRB itself followed by ESah, SSah, and WSah (Figure 6a). It is notable that on days  $-1$  and  $-2$  over the NRB,  $(E - P) > 50$  mm/day, which reduces to a minimum ( $<10$  mm/day) on day  $-10$ . The SATl and NATl sources are moisture sinks until day  $-3$ , but then, up to day  $-10$  both become moisture sources for the NRB. Over the MEDT the moisture uptake increases after day  $-3$  (backwards), which supports the  $(E - P)$  pattern shown in Figure 3. Like the MEDT, EA becomes more important providing moisture during last few days, although it ends up being a less important source in the total daily moisture uptake for the NRB.

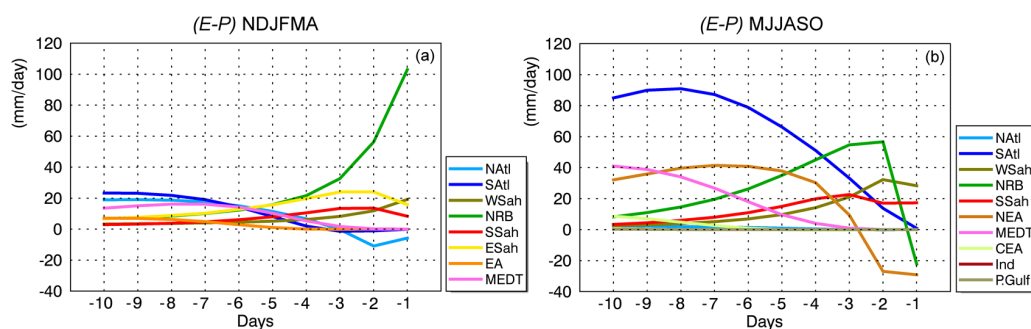


**Figure 6.** Climatological absolute daily (1–10 days) values of  $(E - P)$  integrated using a backward analysis from the NRB considering moisture sources for NDJFMA (a) and MJJASO (b) for the period 1980–2014. The acronyms of the sources regions correspond with those given in Figure 5.

In the wet season when the precipitation over the basin is greater (Figure 7), the NRB acts as a moisture sink on day  $-1$  (Figure 6b). The role of the basin changes from day  $-2$  backwards in time, when it provides humidity for itself and is the most important moisture source until day  $-3$  ( $>50$  mm/day). For SSah and WSah, in the analysis these sources provide moisture to the NRB during all 10 days, being more important during the first days. For both SSah and WSah the  $(E - P) > 0$  values decrease over the last few days of the analysis. After day  $-4$  backwards in time, and in order of importance, the highest moisture uptake takes place over the SATl and NEA. In the wet season SATl becomes the most important moisture source (from day  $-4$  to  $-10$ ) for the NRB. NEA is a moisture sink for the first two days of backwards tracking, in agreement with the pattern of  $(E - P)$  over this region shown in Figure 3 for these days. During last few days (from day  $-6$  backwards), the MEDT is an important moisture source ( $>20$  mm/day) for the NRB. Over the smaller sources of CEA, Indian Ocean, and the Persian Gulf, the air masses in transit to the NRB only gain small amounts of moisture ( $<10$  mm/day). In this season, when the rainfall is intense over the NRB (Figure 7) the moisture uptake

over all days seems to be greater than that obtained for NDJFMA, with the exception of the moisture supply by the NRB itself, which is greater for the first two days during the dry season. Additionally, the resulting  $(E - P)$  over the previously and important Natl moisture source, decreased and becomes one of the less important. As expected in both semi-annual periods NDJFMA and MJJASO, it is notable that the greatest moisture uptake during the first few days backwards in time occurs over the NRB itself, and the surrounding sources, while for the last few days it occurs over the sources furthest away.

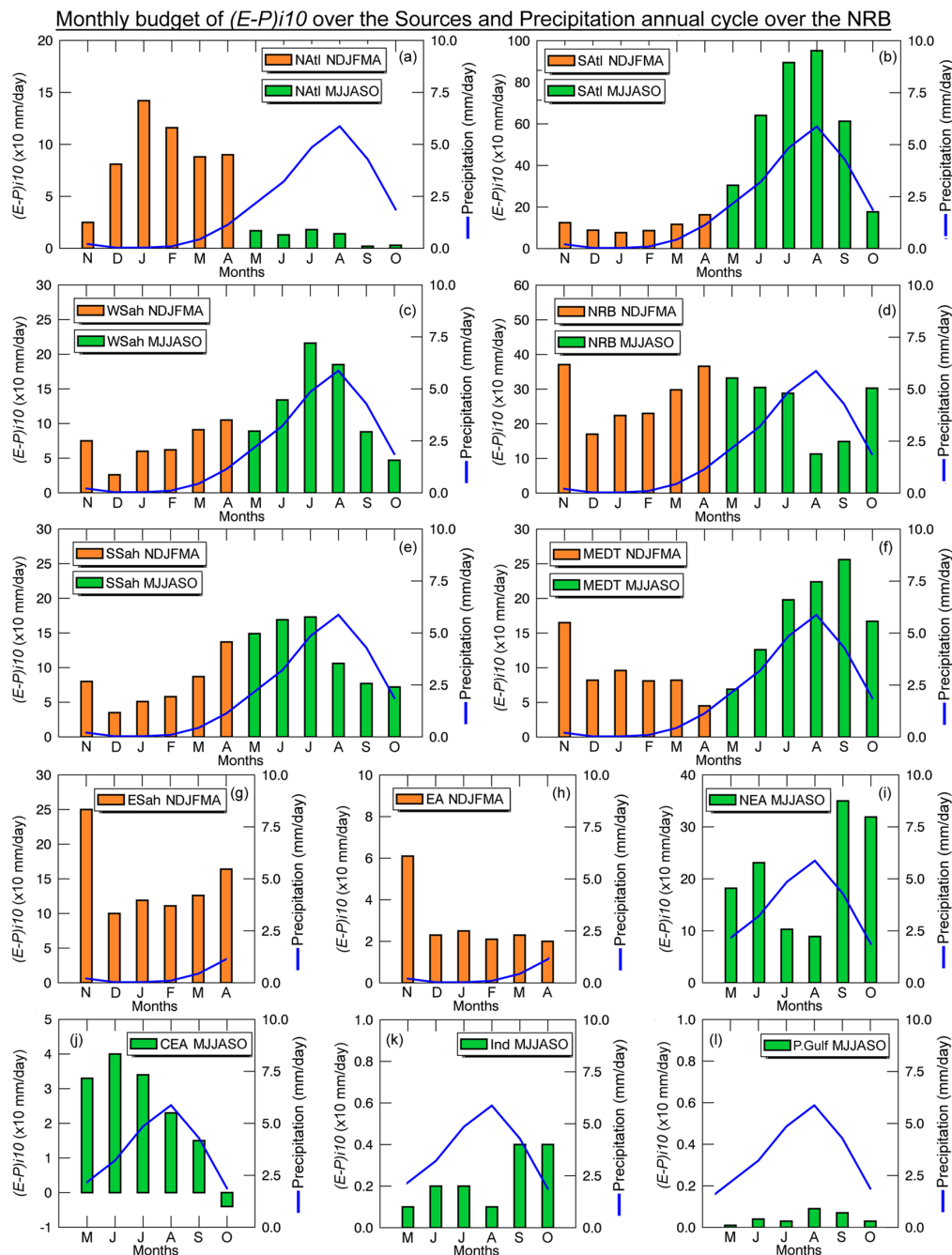


**Figure 7.** Climatological monthly  $(E - P)/10$  values backward integrated from the Niger River Basin over the sources in NDJFMA–MJJASO (bar columns in orange and green, respectively) and precipitation over the NRB (blue line). The acronyms of the sources regions correspond with those given in Figure 5, in the order from (a) to (l).  $(E - P)/10$  from FLEXPART running and precipitation from CRU, for the period 1980–2014.

#### 4.4. Monthly Budget of $(E - P)i10$ over the Sources and Precipitation in the NRB

The moisture sources identification for the Niger catchments by Stohl and James [13] did not explore, but recommended, the analysis of the seasonal and interannual variability in the moisture transport. In this work the source-receptor relationship was also assessed at a monthly scale by calculating the budget of  $(E - P)i10$  over the sources defined for each climatological season. The results are represented in Figure 7 (orange and green columns), together with the annual cycle of precipitation in the NRB (blue line). It is important to note that some of the sources change spatially between the two analysed seasons and others only appear during one of them. Hence, the two coloured bars (orange and green) serve to highlight that although the moisture sources remain within a geographical region they change spatially between NDJFMA and MJJASO (Figure 5).

The spatially-averaged monthly precipitation over the NRB in the first and last months of the year is less than 1 mm/day, but it increases from February until it reaches a maximum in August (5.9 mm/day) (Figure 7) during the African monsoon peak. To support the results in Figure 7 we calculated the mean vertically integrated moisture flux (VIMF) for November–April and May–October, and plotted in the extents of the sources (Figure 5).

Starting with the moisture sources located in the Atlantic Ocean, NATl and SATl (Figure 7a,b, respectively) play different roles over the year. Over NATl the maximum moisture uptake occurs from November to April, when this source is extended to the west over the ocean (Figure 5a), reaching a peak near 150 mm/day in January. In general during these months the VIMF carries humidity from NATl to the northern half of the NRB (Figure 5a), being slightly higher in January (Figure 8a). Climatologically, December, January, and February are the driest months in the basin (Figure 7), but the moisture uptake over NATl is at a maximum in the climatological year. From June to November when the WAM develops and affects WA, this source experiences a spatial reduction (Figure 5b) and with this, a decrease in the monthly average budget of  $(E - P)i10$  in the air masses over it. During this period, the average direction of the VIMF over this region changes to flow from the east (Figure 5b), which does not favour moisture transport from the NATl source to the basin. The monthly annual cycle of the  $(E - P)$  values over this source is clearly opposite to the precipitation cycle in the basin. These results suggest that despite providing moisture to the NRB the NATl is not an effective moisture source for precipitation here during the rainy season.

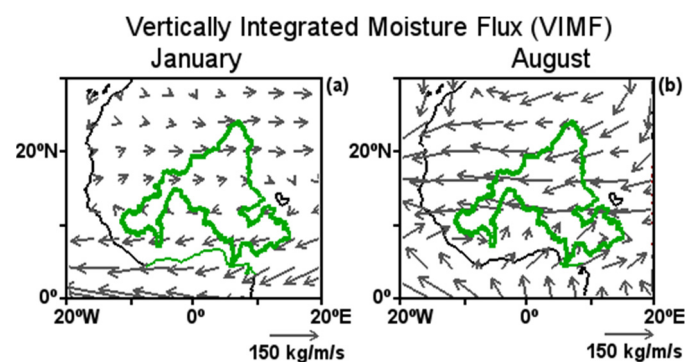


**Figure 8.** Vertically integrated moisture flux (VIMF) climatology for January (a) and August (b). Data from ERA-Interim Reanalysis for 1980–2014.

The SATl source, as might be expected due to its location predominantly south of the equator, has an  $(E - P)i10$  cycle (Figure 7b) opposite to that computed for the NATl source. The budget of  $(E - P)i10$  over the SATl source is positive during all the year and shows values increasing from the dry months until August (when reach > 900 mm/day). From June to September, when the boundaries of this source extend to the south of 30° S (Figure 5b), the moisture uptake over this source is greater than 600 mm/day. This concurs with the penetration of VIMF to the south of the NRB carrying moisture

from the Gulf of Guinea (Figure 5b), which is more appreciable in August (Figure 8b). In general the African Sahel is influenced throughout the monsoon period by southerly winds transporting moisture from the Gulf of Guinea [50]. These results are in agreement with similar findings for the NRB by Stohl and James [13]. The annual cycle of the budget of  $(E - P)i10$  over the SATl source matches the cycle of precipitation over the NRB (Figure 7b), which also agrees with previous results of Gong and Eltahir [1] who argue that moisture fluxes from the tropical Atlantic are almost in phase with rainfall in WA. The maximum precipitation in the NRB occurs in August when the maximum moisture uptake occurs from the SATl source, and less precipitation occurs when the NRB receives less moisture from this oceanic source. Contrary to Natl, this source seems to be very effective for precipitation in the NRB.

The monthly budget of  $(E - P)i10$  over WSah is always positive (Figure 7c), which means that the air masses from here that are in transit to the NRB take up humidity throughout the year. The budget reflects a quite similar cycle to the precipitation over the basin (Figure 7c), similar to SATl. From December to April the moisture uptake increases month by month, decreasing in May, but in July it reaches an annual maximum (>200 mm/day). Regarding the VIMF, it is observed over WSah coming from the west to the east in NDJFMA, carrying moisture to the NRB, and from the east to the west in NJJASO not favouring the moisture supply to the basin.

The only source to be defined without reference to spatial changes over the year is the NRB itself, which is of interest especially in view of its role in providing its own moisture supply. The NRB provides humidity to the atmospheric column in all months of the year (Figure 7d). The annual cycle of  $(E - P)i10$  is characterised by two maxima greater than 350 mm/day in November and April and a minimum in August (<120 mm/day) coinciding with the maximum precipitation rate over the basin. This behaviour confirms the important role of other sources providing moisture for precipitation in the NRB.

To the south of the NRB, the budget of  $(E - P)i10$  over the SSah source is always positive, reaching a maximum of 170 mm/day in July (Figure 7e). The precipitation in the basin seems to show a one-month lag with respect to the budget of  $(E - P)i10$  over the SSah. The VIMF appears towards the west over this region during the dry season while for the wet season it also penetrates in the source from the Gulf of Guinea (Figure 5).

The MEDT source plays a distinct role in the moisture uptake by air masses in transit to the NRB. The budget of  $(E - P)i10$ , with positive values in all months confirms the moisture uptake, which is at a maximum from July to September (Figure 7f) when the precipitation is at a maximum in the basin. Nevertheless, in November when  $(E - P)i10 > 150$  mm/day the precipitation is less than 1 mm/day. In a previous study of the NRB moisture sources, Stohl and James [13] documented that the Mediterranean air masses provide 5% of the NRB precipitation. During the wet season, on average, the VIMF over the Mediterranean region is from the west, but it then forms two branches over this source; one of these flows southwards over northeast Africa before turning westwards reaching the northern half of the NRB (Figure 5b). It is clearly appreciated in August (Figure 8b), the rainiest month in the basin. For NDJFMA it is not clear that the VIMF reaches the NRB from the MEDT source (Figure 5a), which is agreement with the decrease in the  $(E - P)i10$  over it in this season.

The ESah is a source of moisture for the NRB only during the dry season. The budget of  $(E - P)i10$  over this source remain positive during all months and is maximum in November (~250 mm/day) (Figure 7g). The other source for this season, EA, contributes with positive but smaller  $(E - P)i10$  values than those obtained over ESah, with a maximum also in November of around 60 mm/day (Figure 7h). The VIMF from the east has a low magnitude and mostly enters via the southern part of the basin (Figure 5a).

Regarding the sources that only appear in the wet season, NEA (occupying much of northeast Africa) seems to join the regions identified as moisture sources of the NRB during the dry season, ESah and EA. Air masses tracked backwards from the NRB yield a considerable amount of moisture in all months (>80 mm/day) (Figure 7i). In the wet season, the VIMF over NEA reach the basin from the east (Figure 5b). For CEA the budget of  $(E - P)i10$  is negative in October; this implies that air masses tracked

backwards from the NRB, lose rather than gain, humidity over CEA, because it acts as a moisture sink (Figure 7j). In the rest of months the budget is positive but moisture uptake over this source results much less than obtained over the previous described sources. Though from East Africa and Central Africa almost all of the evaporation is recycled regionally or transported to West Africa [8]. Over the Indian Ocean and the Persian Gulf (Figure 7k,l) the budget of  $(E - P)i10$  is positive and small; in fact, Druyan and Koster [4] previously confirmed that Indian Ocean evaporate did not precipitate at all over the Sahel. The findings of the VIMF over these sources appear to advect moisture by the southern border of the NRB (Figure 5b).

#### 4.5. Seasonal $(E - P)i10 > 0$ over the Sources

To summarise the role of each source of moisture for the NRB in both seasons NDJFMA and MJJASO, we calculated the total moisture uptake ( $(E - P)i10 > 0$ ) over the sources and the percentage they represent. The results are expressed in percentage terms in Figure 9. The numbers in the figure relate to inside, or to the nearest possible colour contour representing each source boundary.

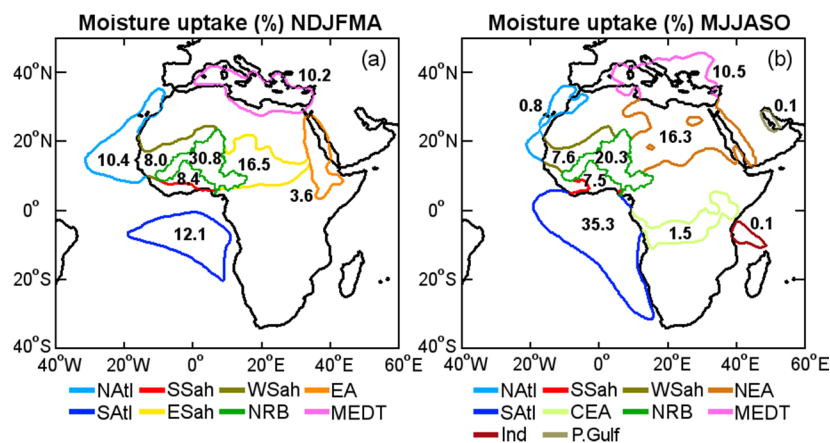


**Figure 9.** Percentage moisture uptake ( $(E - P) > 0$ ) by the NRB over the climatological sources during NDJFMA (a) and MJJASO (b). The colour contours indicates the boundaries of the moisture sources in both seasons.

In NDJFMA (Figure 9a) the NRB itself (30.8%), ESah (16.5%), SATl (12.1%), and the MEDT (10.2%) are the regions where the air masses gained the most moisture for the NRB, while the least important sources are WSah (8.0%) and EA (3.6%). In MJJASO the most important sources are SATl (35.3%), which has a greater extent in this period and the NRB (20.3%), followed by NEA (16.3%) and the MEDT (10.5%) (Figure 9b). The MEDT source (now covering part of the European Mediterranean countries) in this season increase the moisture contribution to the NRB (Figure 7f); nevertheless, it represents almost the same percentage of the total moisture uptake in both seasons. The CEA, NATl, Ind, and P.Gulf sources are the least important; here the uptake represents 1.5%, 0.8%, 0.1%, and 0.1%, respectively, of the total moisture uptake for the air masses travelling towards the NRB.

Focusing on the role of the NRB itself, its own moisture contribution is greater in NDJFMA than in MJJASO, which can be explained by the maximum precipitation seen during the wet season, which favours the loss of moisture. This supports the finding that during the WAM the precipitation in the NRB is fed by moisture transported mainly from SATl, NRB, NEA, and MEDT. These results reveal the importance of moisture contribution by the ocean, even when terrestrial surfaces represent 77% of the Western Sahel precipitation shed and oceanic surfaces comprise the remaining 23% [9]. The seasonal moisture uptake quantification over the moisture sources of the NRB, reveals that largest fraction of moisture income to the basin (69.2% in NDJFMA and 79.7% in MJJASO) comes from outside its boundaries (Figure 9).

## 5. Conclusions

The main moisture sources for the Niger River Basin were investigated during the dry and wet seasons defined at a semi-annual scale, i.e., dry (NDJFMA) and wet (MJJASO). The sources were identified using a Lagrangian approach for 35 years (1980–2014), which ensured reliable climatological results.

- The moisture sources for the NRB in both seasons are located in the tropical east North Atlantic Ocean (NAtl), the tropical east South Atlantic Ocean (SAtl), the surrounding Sahel areas, the Mediterranean region (MEDT), and the NRB itself (Figure 5). They experience differences in the spatial extension between the rainy and dry seasons in the NRB.
- The sources appear during NDJFMA, herein termed ESah and EA, seem to join together in MJJASO occupying north-east Africa (NEA). Additionally, during the wet season three moisture sources appear in central equatorial Africa (CEA), the Indian Ocean (Ind), and on the Persian Gulf (Figure 5).
- Computing the budget of  $(E - P)$  for the air masses tracked up to 10 days backwards in time from the NRB, it was found that the NRB itself, and the surrounding Sahel regions, are mainly responsible for moisture uptake during the first few days of the backwards analysis confirming, as expected from previous studies, the importance of recycling in this region. Further back in time, SAtl, NAtl, NEA, and MEDT are the most important sources (Figures 3 and 6).
- During the dry season, when the precipitation decreases over the basin (Figure 7), the main moisture sources (those where the greatest moisture uptake takes place) are the NRB itself, followed by ESah and SAtl (Figure 9a).
- In the rainy season, together with greater precipitation over the NRB (Figure 7), the  $(E - P)_{i10} > 0$  values over the NRB itself decrease (Figures 7d and 9b). In these months (May–October) the atmospheric circulation associated with the West African monsoon favours greater moisture transport to the basin from regions located to the north-east, east, and south of the basin (Figure 5b).
- The seasonal moisture uptake quantification over the moisture sources of the NRB, reveals that the largest fraction of moisture income to the basin (69.2% in NDJFMA and 79.7% in MJJASO) comes from outside its boundaries (Figure 9). This finding suggests that precipitation variability over the basin must be governed by the moisture contributions from these sources.

It is not always true that more or less moisture uptake over some sources leads to more or less precipitation over the NRB. In fact, the moisture uptake over the NAtl source is greater from November to April when the precipitation is generally less over the NRB, while the opposite tends to apply in the other months. A fact is that the amount of moisture uptake depends of the balance of  $(E - P)$  over the sources because they can act as moisture sinks, as occurs over the CEA in October. These findings suggest that NAtl is not an effective moisture source for rainfall in the NRB. On the contrary, SAtl supplies a great percentage of the total moisture uptake of the basin and exhibits the same annual cycle of the precipitation, suggesting the importance of this oceanic region in supplying moisture for rainfall in the NRB (Figure 7).

Further research to provide new insights into the hydrological cycle in the NRB is underway. This comprises the use of FLEXPART in a forward experiment from each of the sources, which will allow us to investigate the inter-annual variability of the moisture contribution to the basin and establish quantitative relationships with precipitation, including the possible impacts of different modes of climate variability and the role of the sources during drought conditions.

**Supplementary Materials:** The following are available online at [www.mdpi.com/2073-4433/8/2/38/s1](http://www.mdpi.com/2073-4433/8/2/38/s1).

**Acknowledgments:** Rogert Sorí would like to acknowledge funding by the Xunta of Galicia, Spain, in support of this doctoral research; Raquel Nieto acknowledges support from CNPq grant 314734/2014-7 provided by the Brazilian government, and Anita Drumond acknowledges the support of the Spanish Government and FEDER via the SETH (CGL2014-60849-JIN) project.

**Author Contributions:** Rogert Sorí, and Luis Gimeno designed, proposed and conducted the research; Rogert Sorí performed the experiments and analysed the data; Rogert Sorí, Raquel Nieto, Luis Gimeno and Anita Drumond wrote the paper.

**Conflicts of Interest:** The authors declare no conflict of interest. The founding sponsors had no role in the design of the study; in the collection, analyses, or interpretation of data; in the writing of the manuscript, or in the decision to publish the results.

## References

- Gong, C.; Eltahir, E.A.B. Sources of Moisture for Rainfall in West Africa. *Water Resour. Res.* **1996**, *32*, 3115–3121. [[CrossRef](#)]
- Durán-Quesada, A.M.; Gimeno, L.; Amador, J.A.; Nieto, R. Moisture sources for Central America: Identification of moisture sources using a Lagrangian analysis technique. *J. Geophys. Res.* **2010**, *115*, D05103.
- Gimeno, L.; Stohl, A.; Trigo, R.M.; Dominguez, F.; Yoshimura, K.; Yu, L.; Drumond, A.; Durán-Quesada, A.M.; Nieto, R. Oceanic and terrestrial sources of continental precipitation. *Rev. Geophys.* **2012**, *50*, RG4003. [[CrossRef](#)]
- Druyan, L.M.; Koster, R.D. Sources of Sahel Precipitation for Simulated Drought and Rainy Seasons. *J. Clim.* **1989**, *2*, 1438–1446. [[CrossRef](#)]
- Eltahir, E.A.B.; Bras, R.L. Precipitation recycling. *Rev. Geophys.* **1996**, *34*, 367–378. [[CrossRef](#)]
- Nieto, R.; Gimeno, L.; Trigo, R.M. A Lagrangian identification of major sources of Sahel moisture. *Geophys. Res. Lett.* **2006**, *33*, 1–6. [[CrossRef](#)]
- Dirmeyer, P.A.; Brubaker, K.L.; DelSole, T. Import and export of atmospheric water vapor between nations. *J. Hydrol.* **2009**, *365*, 11–22. [[CrossRef](#)]
- Van der Ent, R.J.; Savenije, H.H.G.; Schaeffli, B.; Steele-Dunne, S.C. Origin and fate of atmospheric moisture over continents. *Water Resour. Res.* **2010**, *46*, W09525. [[CrossRef](#)]
- Keys, P.W.; van der Ent, R.J.; Gordon, L.J.; Hoff, H.; Nikoli, R.; Savenije, H.H.G. Analyzing precipitationsheds to understand the vulnerability of rainfall dependent regions. *Biogeosciences* **2012**, *9*, 733–746. [[CrossRef](#)]
- Keys, P.W.; Barnes, E.A.; van der Ent, R.J.; Gordon, L.J. Variability of moisture recycling using a precipitationshed framework. *Hydrol. Earth Syst. Sci.* **2014**, *18*, 3937–3950. [[CrossRef](#)]
- Goessling, H.F.; Reick, C.H. On the “well-mixed” assumption and numerical 2-D tracing of atmospheric moisture, *Atmos. Chem. Phys.* **2013**, *13*, 5567–5585.
- Arnault, J.; Knoche, R.; Wei, J.; Kunstmann, H. Evaporation tagging and atmospheric water budget analysis with WRF: A regional precipitation recycling study for West Africa. *Water Resour. Res.* **2016**, *52*, 1544–1567. [[CrossRef](#)]
- Stohl, A.; James, P. A Lagrangian analysis of the atmospheric branch of the global water cycle: 2. Earth’s river catchments, ocean basins, and moisture transports between them. *J. Hydrometeorol.* **2005**, *6*, 961–984. [[CrossRef](#)]
- The Center for Ocean-Land-Atmosphere Studies. Available online: <http://cola.gmu.edu/wcr/river/Niger.png> (accessed on 2 February 2017).
- Liebmann, B.; Blade, I.; Kiladis, G.N.; Carvallo, L.M.V.; Senay, G.B.; Allured, D.; Leroux, S.; Funk, C. Seasonality of African Precipitation from 1996 to 2009. *J. Clim.* **2011**, *25*, 4304–4322. [[CrossRef](#)]
- Biasutti, M.; Yuter, S.E. Observed frequency and intensity of tropical precipitation from instantaneous estimates. *J. Geophys. Res. Atmos.* **2013**, *118*, 9534–9551. [[CrossRef](#)]
- Niang, I.; Ruppel, O.C.; Abdrabo, M.A.; Essel, A.; Lennard, C.; Padgham, J.; Urquhart, P. Africa. In *Climate Change 2014: Impacts, Adaptation, and Vulnerability. Part B: Regional Aspects; Contribution of Working Group II to the Fifth Assessment Report of the Intergovernmental Panel on Climate Change*; Cambridge University Press: Cambridge, UK, 2014; pp. 1199–1265.
- Nicholson, S.E.; Some, B.; Kone, B. An analysis of recent rainfall conditions in West Africa, including the rainy seasons of the 1997 El Nino and the 1998 La Nina years. *J. Clim.* **2000**, *13*, 2628–2640. [[CrossRef](#)]
- Lebel, T.; Ali, A. Recent trends in the Central and Western Sahel rainfall regime (1990–2007). *J. Hydrol.* **2009**, *375*, 52–64. [[CrossRef](#)]
- Huang, J.; Zhang, C.; Prospero, J.M. Large-scale effect of aerosols on precipitation in the West African Monsoon region. *Q. J. R. Meteorol. Soc.* **2009**, *135*, 581–594. [[CrossRef](#)]

21. Djebou, D.C.S. Integrated approach to assessing streamflow and precipitation alterations under environmental change: Application in the Niger River Basin. *J. Hydrol. Reg. Stud.* **2015**, *4*, 571–582. [[CrossRef](#)]
22. Nicholson, S.E. The West African Sahel: A Review of Recent Studies on the Rainfall Regime and Its Interannual Variability. *ISRN Meteorol.* **2013**, *2013*, 1–32. [[CrossRef](#)]
23. The Niger River Basin Authority (NBA). Executive Secretariat P.O.Box 729, Niamey (Niger). Available online: <http://www.abn.ne> (accessed on 1 November 2016).
24. Ogilvie, A.; Mahe, G.; Ward, J.; Serpantie, G.; Lemoalle, J.; Morand, P.; Barbier, B.; Diop, A.T.; Caron, A.; Namara, R.; et al. Water, agriculture and poverty in the Niger River Basin. *Water Inter.* **2010**, *35*, 594–622. [[CrossRef](#)]
25. Buontempo, C. *Sahelian Climate: Past, Current, Projections*; Sahel and Club West Africa Secretariat. Met Office Hadley Centre: London, UK, 2010; pp. 1–20.
26. L'Hôte, Y.; Mahé, G. *Afrique de l'ouest et Centrale. Carte des Précipitations Moyennes Annuelles (Période 1951–1989)*; Office de la Recherche Scientifique et Technique d'Outre-Mer (ORSTOM): Paris, France, 1996. (In French)
27. Andersen, I.; Dione, O.; Jarosewich-Holder, M.; Olivry, J.-C. *The Niger River Basin: A Vision for Sustainable Management*; World Bank: Washington, DC, USA, 2005.
28. Van der Ent, R.J. A New View on the Hydrological Cycle over Continents. Ph.D. Thesis, Delft University of Technology, Delft, The Netherlands, 2014.
29. Nicholson, S. On the question of the “recovery” of the rains in the West African Sahel. *J. Arid Environ.* **2005**, *63*, 615–641. [[CrossRef](#)]
30. Knippertz, P.; Andreas, H.F. Dry-Season Precipitation in Tropical West Africa and Its Relation to Forcing from the Extratropics. *Mon. Weather Rev.* **2008**, *136*, 3579–3596. [[CrossRef](#)]
31. Lavaysse, C.; Flamant, C.; Janicot, S.; Parker, D.J.; Lafore, J.-P.; Sultan, B.; Pelon, J. Seasonal evolution of the West African heat low: A climatological perspective. *Clim. Dyn.* **2009**, *33*, 313–330. [[CrossRef](#)]
32. Lavaysse, C.; Flamant, C.; Evan, A.; Janicot, S.; Gaetani, M. Recent climatological trend of the Saharan heat low and its impact on the West African climate. *Clim. Dyn.* **2015**. [[CrossRef](#)]
33. Sultan, B.; Janicot, S. The West African Monsoon Dynamics. Part II: The “Preonset” and “Onset” of the Summer Monsoon. *J. Clim.* **2003**, *16*, 3407–3427. [[CrossRef](#)]
34. Namara, R.E.; Barry, B.; Owusu, E.S.; Ogilvie, A. *An Overview of the Development Challenges and Constraints of the Niger Basin and Possible Intervention Strategies*; IWMI Working Paper 144; International Water Management Institute: Colombo, Sri Lanka, 2011; pp. 1–34. [[CrossRef](#)]
35. Zhang, C.; Woodworth, P.; Gu, G. The seasonal cycle in the lower troposphere over West Africa from sounding observations. *Q. J. R. Meteorol. Soc.* **2006**, *132*, 2559–2582. [[CrossRef](#)]
36. Stohl, A.; James, P. A Lagrangian analysis of the atmospheric branch of the global water cycle. Part 1: Method description, validation, and demonstration for the August 2002 flooding in central Europe. *J. Hydrometeorol.* **2004**, *5*, 656–678. [[CrossRef](#)]
37. Numaguti, A. Origin and recycling processes of precipitating water over the Eurasian continent: Experiments using an atmospheric general circulation model. *J. Geophys. Res.* **1999**, *104*, 1957–1972. [[CrossRef](#)]
38. Salih, A.A.M.; Zhang, Q.; Tjernström, M. Lagrangian tracing of Sahelian Sudan moisture sources. *J. Geophys. Res. Atmos.* **2015**, *120*, 6793–6808. [[CrossRef](#)]
39. Nieto, R.; Gallego, D.; Trigo, R.M.; Ribera, P.; Gimeno, L. Dynamic identification of moisture sources in the Orinoco basin in equatorial South America. *Hydrol. Sci. J.* **2008**, *53*, 602–617. [[CrossRef](#)]
40. Drumond, A.; Nieto, R.; Gimeno, L. Sources of moisture for China and their variations during drier and wetter conditions in 2000–2004: A Lagrangian approach. *Clim. Res.* **2011**, *50*, 215–225. [[CrossRef](#)]
41. Drumond, A.; Marengo, J.; Ambrizzi, T.; Nieto, R.; Moreira, L.; Gimeno, L. The role of the Amazon Basin moisture in the atmospheric branch of the hydrological cycle: A Lagrangian analysis. *Hydrol. Earth Syst. Sci.* **2014**, *18*, 2577–2598. [[CrossRef](#)]
42. Nieto, R.; Castillo, R.; Drumond, A.; Gimeno, L. A catalog of moisture sources for continental climatic regions. *Water Resour. Res.* **2014**, *50*, 5322–5328. [[CrossRef](#)]
43. Drumond, A.; Taboada, E.; Nieto, R.; Gimeno, L.; Vicente-Serrano, S.M.; López-Moreno, J.I. A Lagrangian analysis of the present-day sources of moisture for major ice-core sites. *Earth Syst. Dynam.* **2016**, *7*, 549–558. [[CrossRef](#)]

44. Drumond, A.; Nieto, R.; Gimeno, L. A Lagrangian approach for investigating anomalies in the moisture transport during drought episodes. *Cuad. Investig. Geogr.* **2016**, *42*, 113–125. [[CrossRef](#)]
45. Dee, D.P.; Uppala, S.M.; Simmons, A.J.; Berrisford, P.; Poli, P.; Kobayashi, S.; Andrae, U.; Balmaseda, M.A.; Balsamo, G.; Bauer, P.; et al. The ERA-Interim reanalysis: Configuration and performance of the data assimilation system. *Q. J. R. Meteorol. Soc.* **2011**, *137*, 553–597. [[CrossRef](#)]
46. Harris, I.; Jones, P.D.; Osborn, T.J.; Lister, D.H. Updated high-resolution grids of monthly climatic observations—The CRU TS3.10 Dataset. *Int. J. Climatol.* **2014**, *34*, 623–642. [[CrossRef](#)]
47. Schicker, I.; Radanovics, S.; Seibert, P. Origin and transport of Mediterranean moisture and air. *Atmos. Chem. Phys.* **2010**, *10*, 5089–5105. [[CrossRef](#)]
48. Levine, R.C.; Turner, A.G. Dependence of Indian monsoon rainfall on moisture fluxes across the Arabian Sea and the impact of coupled model sea surface temperature biases. *Clim. Dyn.* **2012**, *38*, 2167–2190. [[CrossRef](#)]
49. Drumond, A.; Nieto, R.; Hernandez, E.; Gimeno, L. A Lagrangian analysis of the variation in moisture sources related to drier and wetter conditions in regions around the Mediterranean Basin. *Nat. Hazards Earth Syst. Sci.* **2011**, *11*, 2307–2320. [[CrossRef](#)]
50. Lélé, M.I.; Leslie, L.M.; Lam, P.J. Analysis of Low-Level Atmospheric Moisture Transport Associated with the West African Monsoon. *J. Clim.* **2015**, *28*, 4414–4430. [[CrossRef](#)]



© 2017 by the authors; licensee MDPI, Basel, Switzerland. This article is an open access article distributed under the terms and conditions of the Creative Commons Attribution (CC BY) license (<http://creativecommons.org/licenses/by/4.0/>).